

# Thrust Characteristics of Pure Magnetic Sail in Laboratory Experiment

**IEPC-2009-011**

*Presented at the 31st International Electric Propulsion Conference,  
University of Michigan • Ann Arbor, Michigan • USA  
September 20 – 24, 2009*

Kazuma Ueno<sup>1</sup>

*The Graduate University for Advanced Studies, Sagamihara, Kanagawa, 229-8510, Japan*

Ikkoh Funaki<sup>2</sup>

*Japan Aerospace Exploration Agency, Sagamihara, Kanagawa, 229-8510, Japan*

Yuya Oshio<sup>3</sup>

*The Graduate University for Advanced Studies, Sagamihara, Kanagawa, 229-8510, Japan*

Hideyuki Horisawa<sup>4</sup>

*Tokai University, Hiratsuka, Kanagawa, 259-1292, Japan*

*and*

Hiroshi Yamakawa<sup>5</sup>

*Kyoto University, Uji, Kyoto, 611-0011, Japan*

**Abstract: Pure Magnetic Sail (MagSail) is a useful propulsion system utilizing the solar wind, one of the natural energy from the sun, for deep space**

<sup>1</sup> Graduate Student, Department of Space and Astronautical Science, k-ueno@isas.jaxa.jp.

<sup>2</sup> Associate Professor, Institute of Space and Astronautical Science, funaki@isas.jaxa.jp.

<sup>3</sup> Graduate Student, Department of Space and Astronautical Science, oshio@isas.jaxa.jp.

<sup>4</sup> Professor, Department of Aeronautics and Astronautics, horisawa@tokai.ac.jp.

<sup>5</sup> Professor, Research Institute for Sustainable Humanosphere, yamakawa@rish.kyoto-u.ac.jp.

mission. MagSail is accelerated by capturing the solar wind with a magnetic field produced by a coil equipped on the spacecraft. In order to know thrust performance of MagSail, laboratory experiment of MagSail is conducted and magnetic field and thrust were measured. From these results, it is found that asymmetrical shape of magnetopause was observed and thrust increasing for enlargement of magnetic cavity size was confirmed.

### Nomenclature

$B$	= magnetic flux density, T
$B_0$	= initial magnetic flux density of coil, T
$B_{center}$	= magnetic flux density at the center of coil, T
$C_d$	= thrust coefficient
$c$	= light velocity ( $3.0 \times 10^8$ m/s)
$e$	= elementary charge ( $1.6 \times 10^{-19}$ C)
$F$	= thrust, N
$L$	= standoff distance of magnetic cavity, m
$M_d$	= magnetic moment, $\text{Tm}^3$
$M$	= ion Mach number
$m_i$	= mass of proton ( $1.67 \times 10^{-27}$ kg)
$n$	= number density, $\text{m}^{-3}$
$r_{Li}$	= ion Larmor radius, m
$Rm$	= magnetic Reynold's number
$S$	= representative area of magnetic cavity, $\text{m}^2$
$u$	= velocity, m/s
$\delta$	= skin depth, m
$\mu_0$	= permeability in vacuum ( $1.26 \times 10^{-6}$ H/m)
$\sigma$	= electric conductivity, $1/\Omega\text{m}$
$\omega_p$	= plasma frequency, Hz

### Subscripts

$i$	= ion
$mp$	= magnetopause
$sw$	= solar wind

## I. Introduction

**M**agnetic sail (MagSail) is propulsion system propelled by capturing the solar wind toward leaving the sun. The solar wind is high-speed flow of charged particles (ion/electron) jetted from the sun. MagSail has a hoop coil and the coil produces a magnetic field around a spacecraft to receive the solar wind. When the solar wind is interacted with the magnetic field, a magnetosphere is formed around the spacecraft due to the interaction (Figure. 1). That scale of the interaction between the solar wind and the magnetic field determines thrust of MagSail because momentum loss of the solar wind plasma by the interaction is transmitted to the force exerting on the coil. MagSail does not use any propellant for main thrust without attitude controls because main resource of thrust power is the sun energy. Zubrin, a proposer of MagSail, estimated that 20-N-class MagSail needs making a 100-km-diameter blocking area due to the low-density of the solar wind. Recently, new concepts of propulsion systems utilizing the solar wind were proposed and have been studied. Mini-magnetospheric Plasma Propulsion (M2P2) or Magnetoplasma Sail is use an expanded coil magnetic field by plasma injection from the coil inner for the capturing the solar wind. These mechanisms of expansion are now discussing by researchers due to multi-scale physics of the phenomena. In order to evaluate the performance of MPS, at first, we conduct characterization of MagSail.

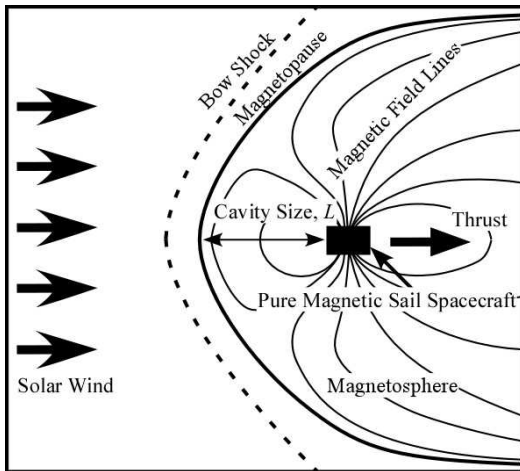


**Figure. 1** Schematics of Pure Magnetic Sail.

## II. Thrust of MagSail and Scaling Parameters

### A. Thrust Exerting on pure MagSail

The force on the current loop depends on the area that blocks the solar wind. By increasing this blocking area, a larger thrust is obtained. Therefore, the force exerting on the coil of the MagSail,  $F$ , can be formulated as<sup>i</sup>,

$$F = C_d \frac{1}{2} \rho u_{sw}^2 S \quad (1)$$

where  $1/2 \rho u_{sw}^2$  the dynamic pressure of the solar wind, and  $S = \pi L^2$  the characteristic area of the magnetosphere.

## B. Definition of Magnetic Cavity Size, Ion Larmor Radius, and Skin Depth

Because the density of the solar wind plasma flow around a Magsail is very small, the charged particles are collision-less and their movement separates the plasma region outside the magnetic cavity and the region inside the magnetic cavity. Simplified picture of this boundary is depicted in Figure. 1. When a magnetic dipole  $M_d$  is located at the center, there is a balance between the total internal (magnetic) and the external (plasma) pressures at the boundary:

$$nm_i u_{sw}^2 = \frac{(2B_{mp})^2}{2\mu_0} \quad (2)$$

where  $2B_{mp}$  the magnetic flux density at the boundary. The magnetic flux density  $B_{mp}$  at a distance  $L$  from the dipole center is expressed as,

$$B_{mp} = \frac{M_d}{4\pi L^3} \quad (3)$$

hence the detachment distance of the boundary from the dipole center,  $L$ , is derived as follows.

$$L = \left( \frac{M_d^2}{8\pi^2 \mu_0 n m_i u_{sw}^2} \right)^{1/6} \quad (4)$$

This boundary is usually called a magnetopause, on which the charged particles, ions and electrons, impinge. The external space is considered as magnetic field-free. In the idealized situation, it is found that the thickness of the magnetopause is the order of the plasma skin depth  $\delta$  as

$$\delta = c / \omega_p \quad (5)$$

where  $c$  is the light velocity, and  $\omega_p$  the plasma frequency. The thickness of the magnetopause, however, is considered larger than  $\delta$ ; it is about the ion gyration radius at the magnetopause<sup>ii</sup>:

$$r_{Li} = \frac{m_i u_{sw}}{e 2 B_{mp}} \quad (6)$$

Because of their heavier mass, the ions tend to penetrate more deeply into the magnetic field than electrons. This sets up a charge separation, thus the outward pointing polarization field restrains the ions. Before the ions can be deflected by the magnetic field, they are returned by this polarization field. The electrons, however, experience the Lorentz force and gain energy in the polarization field. The transverse velocity component of the electrons accounts essentially for the electric current in the interface, which in case of the magnetopause is usually referred to as Chapman-Ferraro current. From Eqs.(5) and (6),  $\delta \sim 1$  km and  $r_{Li} = 72$  km for the solar wind flow in Table. 1.

**Table. 1 Scaling Parameters of MagSail.**

	MagSail in space	Laboratory Design target
Size of magnetic cavity (stand-off distance), $L$	$\sim 200$ km	$\sim 0.1$ m
Thrust of MagSail, $F$ , N	$< 200$	$\sim 1$
Ratio of ion Larmor radius to $L$ , $r_{Li}/L$	0.1-1	0.1-1
Ratio of thickness of magnetopause to $L$ , $\delta/L$	$< 0.01$	$< 0.3$
Magnetic Reynolds number, $Rm$	$> 10^8$	3-15
Mach number	8	1-5

### C. Non-dimensional Parameters

The solar wind is a super sonic plasma flow which consists of collisionless particles. These features are described by the Mach number,  $M > 1$  as well as the magnetic Reynolds number,  $Rm = \sigma \mu_0 u_{sw} L \gg 1$ . Incorporating typical plasma velocity and temperatures of the solar wind,  $M \sim 8$ . In addition to these two scaling parameters, we defined  $r_{Li}/L$ , and  $\delta/L$ , hence four non-dimensional parameters in total are introduced. Among them, the parameters  $Rm$ ,  $r_{Li}/L$ , and  $\delta/L$ , are dominated by the size of the magnetosphere, which was selected as  $L < 200$  km in our preliminary study (see Table. 1). Corresponding non-dimensional parameters are  $0.1 < r_{Li}/L < 1$  (the ion gyration radius is comparable to or larger than  $L$ , which is in contrast to the MHD scale requiring  $r_{Li}/L \ll 1$  in the scaling parameters of geophysics<sup>iii,iv</sup>) and  $\delta < 0.03$  (the skin depth is much smaller than  $L$ ). If the thickness of the magnetopause is small enough in comparison to  $L$ , almost all of the incident ions are reflected at the magnetospheric boundary, hence large thrust on the coil of the MagSail is expected. Vice versa, if the thickness of the magnetopause is much larger than  $L$ , no interaction between the plasma flow and the magnetic field is anticipated. We treat a transitional region from the MHD scale (thin magnetopause mode) to the ion kinetic scale (thick magnetopause mode) in this experiment.

## III. Experimental Setup

To simulate the interaction between a solar wind and a magnetic field of MagSail in laboratory, Magnetic Sail ground simulator which consisted of a solar wind simulator (SWS) and a magnetic sail simulator (MSS), was developed at  $\phi 2.5$  m $\times$ 5 m vacuum chamber shown in Figure. 2. Those simulators

are adjusted to achieve a short steady state operation (~1 ms) and also measurement instructions are synchronized with the ignition of the simulator.

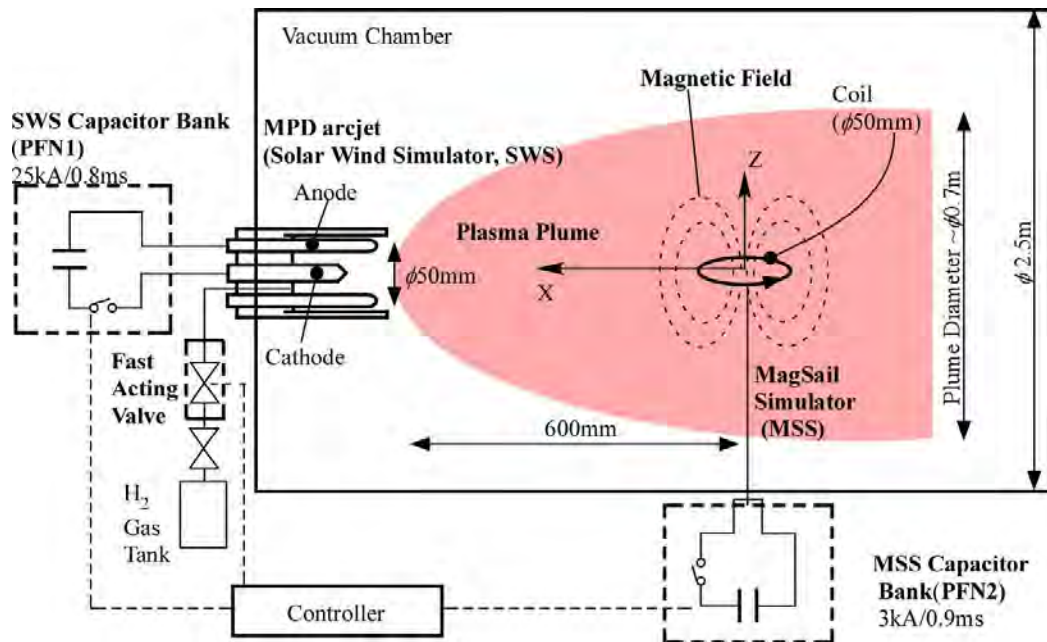


**Figure. 2** Experimental apparatus of Pure Magnetic Sail scale model experiment.

### A. Solar Wind Simulator and MagSail Simulator

Hydrogen magnetoplasmadynamic (MPD) arcjet was selected as the SWS to produce high-speed and high-density plasma simulating the solar wind. The MPD arcjet was constructed of a cathode and 8-anodes located in azimuthally to achieve large diameter plasma plume. The discharge chamber of the MPD arcjet is attached on the chamber inner wall.

A fast-acting valve (FAV) supplies hydrogen gas to gas exhausts located in the cathode root of the MPD arcjet. The mass flow rate was controlled by reservoir pressures and a gas pulse of 8 ms duration was achieved in the discharge chamber.

A pulse-forming network arranging to 0.8 ms-steady state drive supplies max 20-kA discharge current to the discharge chamber. The PFN for the SWS (PFN1) is ignited by a trigger coordinated with the flat-top of gas pulse from a controller. Hydrogen plasma, velocity of 42 km/s and density of  $1.2 \times 10^{19} \text{ m}^{-3}$ , was supplied at 600 mm from the MPD head by the ignition of the MPD arcjet. Typical plasma plume of the SWS is shown in Figure. 4.

$\phi 50$  mm-coil of 20 turns-copper wires is used for simulating of a Magnetic Sail in laboratory, showed in Figure. 5. The coil is immersed into the simulated solar wind at 600 mm from the SWS. The PFN for the MSS (PFN2) supplies coil current below 2 kA before firing of the SWS.

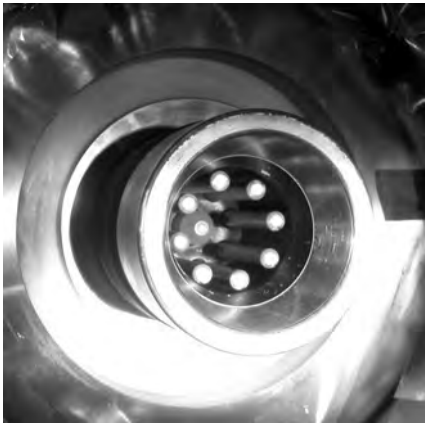


**Figure. 3 Hydrogen Magneto-plasmadynamic arcjet of Solar Wind Simulator.**



**Figure. 4 Typical operation of the solar wind simulator.**

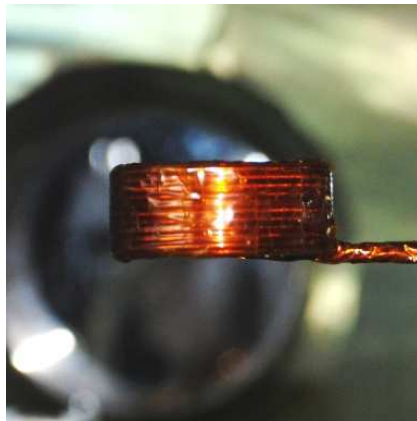


**Figure. 5  $\phi$ 50mm-copper-coil of Magnetic Sail.**

### **B. Thrust Measurement**

Thrust measurements are carried out by the parallelogram-pendulum method. The coil simulating MagSail was mounted on a thrust stand suspended with four steel wires (Figure. 6). The impulse was found from the maximum amplitude of its swing; after subtracting cold impulse bit, it was transformed into thrust by dividing the quasi-steady duration. The displacement of the pendulum was measured with a laser position sensor. For the calibration of the pendulum and position sensor combination, impulses of known magnitude were applied to the target of the thruster. A simple pendulum consisting of a steel ball and a string was used in an atmospheric pressure environment, and the impulses of the ball were calculated from its mass and striking velocity evaluated from the energy conservation for the calibration pendulum. Due to uncertainty of the estimated velocity, the impulse measurement was accurate to within 1%. Major errors in the thrust comes from electromagnetic noise while starting up the discharge of the coil, however, they were less than 20% of the averaged value.

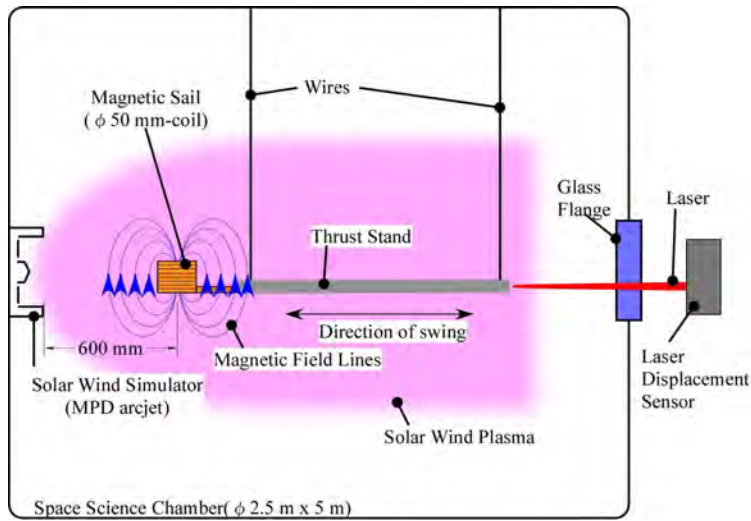


**Figure. 6 Setup of thrust measurement of Magnetic Sail.**

### C. Magnetic field measurement

A three-component magnetic probe consists of  $\phi 0.2$  mm-wire coils (20 turns) twisted on 10-mm cubic probe head, is mounted on a freely-movable stage in three axes by remote control. Output voltages of the coils were integrated analogically during 0.6 ms duration from 0.5 ms with the RC integration circuit and the integrated signals were stored in the digital oscilloscope after amplifying 100-fold. For the calibration of the magnetic probe and the analogical integration circuit, a magnetic field of known flux density was applied to the each coils of the probe. Total magnetic flux density was calculated from three-component synthesis of measured magnetic flux densities with the magnetic probe. To obtain a distribution of magnetic flux density, the probe was moved at different point for each SWS firing using the stage controlled from outside of the chamber.

A structure of magnetic field of MagSail which interacted with the solar wind can be predicted from the structure of geo-magnetosphere. When charge particles feel the coil magnetic field, the particles are vended to opposite directions by Lorentz force and these different motions of the particles make a current which divide the solar wind plasma region and magnetic field region, showed in Figure. 7 a). The current is called magnetopause current and the region of current flow is called magnetopause. Figure. 7 b) shows magnetic field distribution along this line when the magnetic field is interacted with the solar wind. The magnetopause current produces the magnetic field and the induced magnetic field enhances the initial coil magnetic field in the magnetic field region and reduces the initial coil magnetic field in the solar wind region. For example, in the case of geo-magnetic field, the magnetic field is twice as large as the original geo-magnetic field. In the result of the interaction between the solar wind and the magnetic field, the line of interacted magnetic field intersects the line of coil magnetic field. In this study, magnetosphere size  $L$  is defied as the distance from coil center to this crossover point.

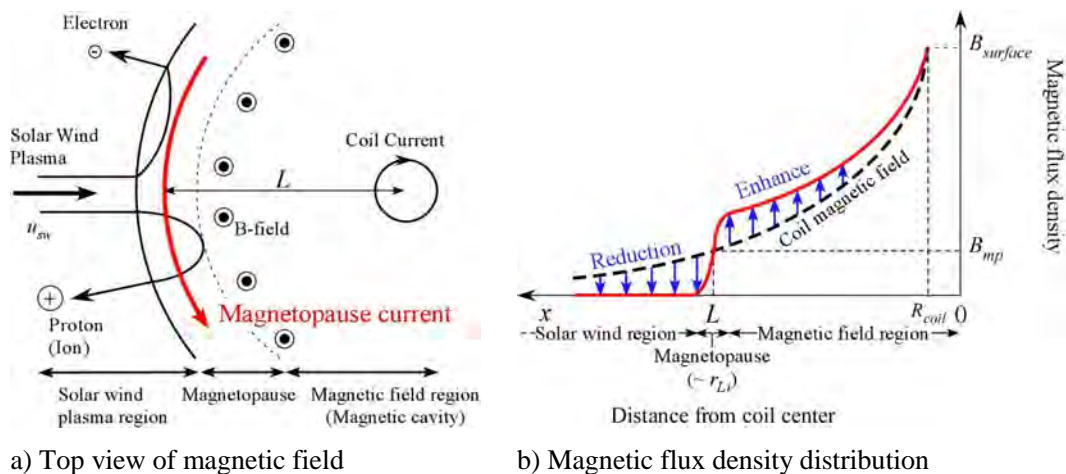


**Figure. 7 Top view of behavior of charge particles invading the magnetic field and magnetic field distribution at that time.**

#### IV. Experimental Results and Discussion

Typical image of the interaction between the solar wind and the magnetic field is shown in Figure. 8. The simulated solar wind plasma came from the left side of the image and a characteristic flow caused by the interaction between the plasma flow and the coil magnetic field was found in the image of overview and close-up. Figure. 9 shows the change of flow fields for changing of the coil current (0, 1, 2 kA). In the case of 0 kA-coil current, uniform plasma flow in front of the coil and a light emission in surface of the coil were observed. In comparison with Figure. 9 a) 0 kA and b) 1kA, it is found that the solar wind flow was effectively blocked by the coil magnetic field. The interaction was obviously enlarged for more increasing of the coil current showed in Figure. 9 c). In addition, the light emission region around the coil was slightly changed by the changing of the coil current. In both b) and c) of Figure. 9, you can find the emission along the magnetic field lines and the emission region in the case of weak magnetic field (b) of Figure. 9) was larger than other cases. Difference of ion Larmor radius due to the difference of magnetic field strength may cause this difference of the emission.

In order to know a size of magnetic cavity, magnetic field for 2 kA-coil current were measured along the lines showed in Figure. 10 a) and b). Normalized magnetic field is showed in Figure. 11 to easily understand a change of the magnetic field. Normalized magnetic field indicates change from the coil magnetic field without the solar wind, described as  $B/B_0$ . You can see the characteristic distribution in Figure. 11 a) which is similar to theoretical distribution of the interaction showed in Figure. 7 b). Thus, magnetic cavity size  $L$  is found as  $L=120$  mm from Figure. 11 a). Here, theoretical size of the magnetic cavity is  $L= 118$  mm using theoretical expression of magnetic cavity described as Eq. (4) and  $u_{sw}=42$  km/s,  $n=1.2 \times 10^{19} \text{ m}^{-3}$ ,  $I=2$  kA of  $\phi 50$  mm and 20 turns-coil. Compared with the measured cavity size, the theoretical size was agreement with the observed size in X-axis. From this agreement, it is found that the changing of the flow field was caused by the changing of the magnetic field.

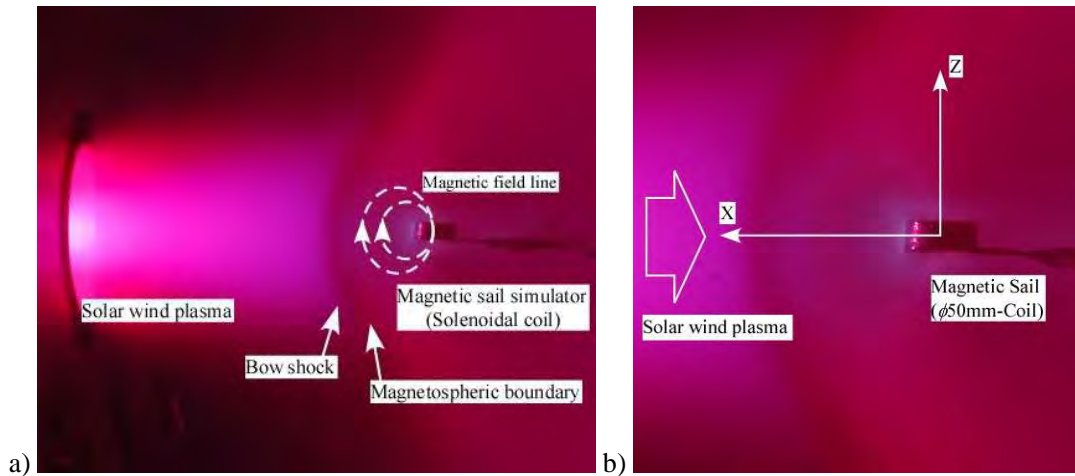


**Figure. 8** CCD image of plasma flow around Magnetic Sail, a) Overview, b) Close-up.

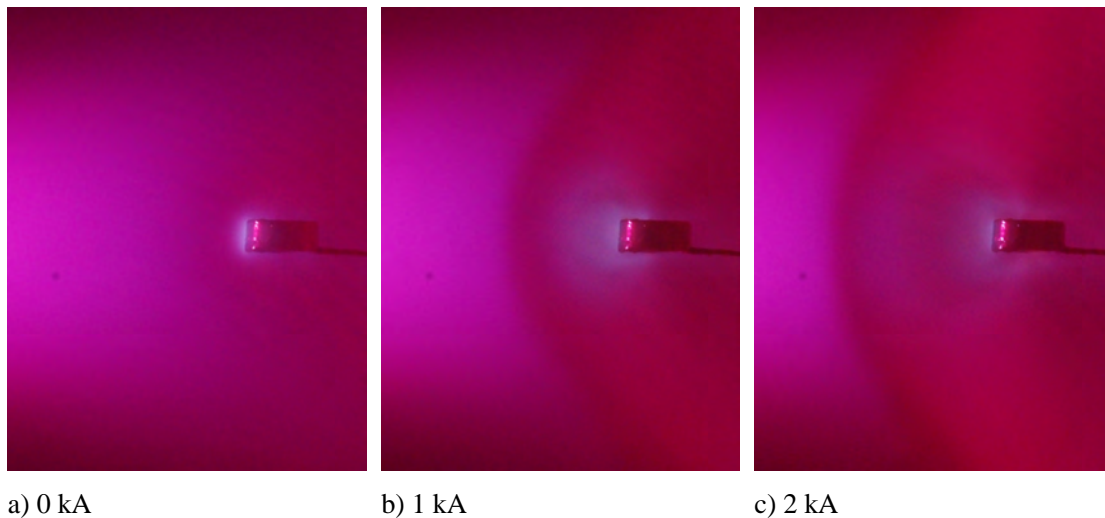
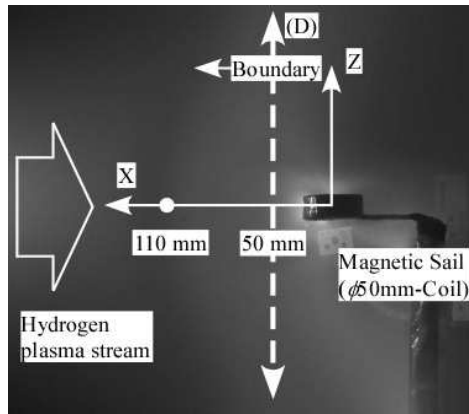


**Figure. 9** Change of flow field for 0, 1, 2 kA-coil current.

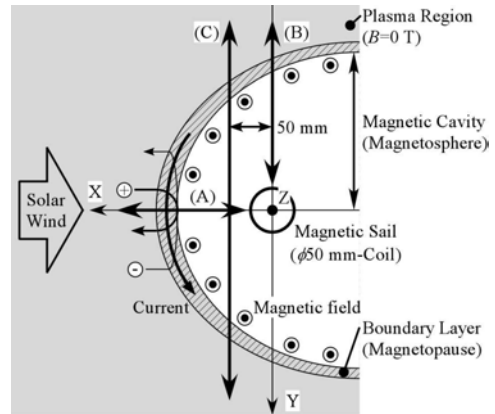
Drastically reduction of magnetic flux density at the region far from the coil center was observed in Figure. 11 (c) and (d). Such a region of weak magnetic field is the plasma region. Hence, the region of magnetic cavity is from  $Y=-110$  to  $180$  mm in Figure. 11 (c) and from  $Z=-180$  to  $180$  mm in Figure. 11 (d). Although the symmetrical magnetic cavity was observed in Z-axis (Figure. 11 (d)), it is found that the asymmetrical magnetic cavity was formed in Y-axis (Figure. 11 (c)). Influence of this kind of asymmetrical magnetic fields on thrust should be investigated to realization of MagSails in the near future.

The results of thrust measurement for several theoretical magnetic cavity sizes from the coil currents (0, 0.3, 0.7, 1.0, 1.3, 1.7, 2.0 kA) are plotted in Figure. 12. It is obviously found that thrust is increased when the magnetic cavity size is enlarged from 64 to 118 mm, but for the large cavity size ( $L > 100$  mm), the thrust values scatter around 1.2 N due to large electromagnetic noises at the highest coil current.

In Figure. 13, thrust coefficients obtained from the Fujita's formula and the experimental results are plotted. We can see that the measured thrust is similar to the theoretical predictions but large error exist.

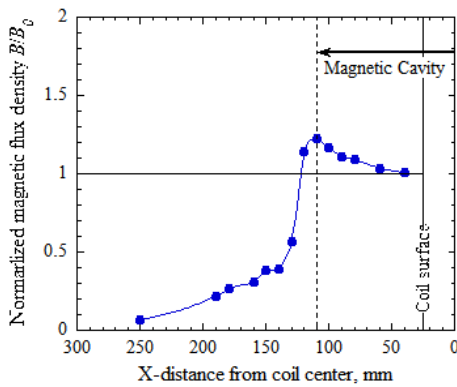


a) Side-view (D)

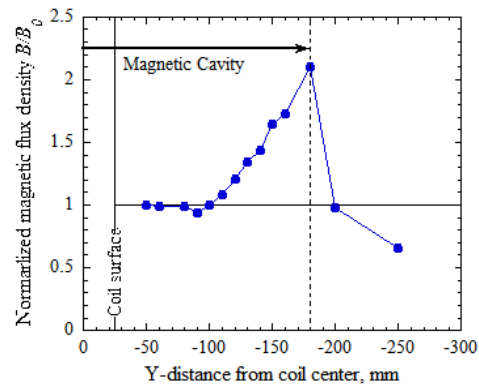


b) Top-view (A, B, C)

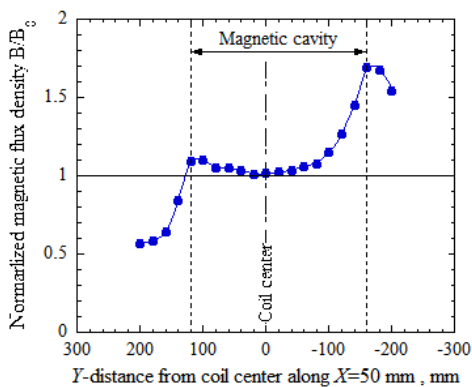
**Figure. 10** Measurement position of magnetic flux density; (A):  $Y=0$  mm,  $Z=0$  mm, (B):  $X=0$  mm,  $Z=0$  mm, (C):  $X=50$  mm,  $Z=0$  mm, (D):  $X=50$  mm,  $Y=0$  mm.



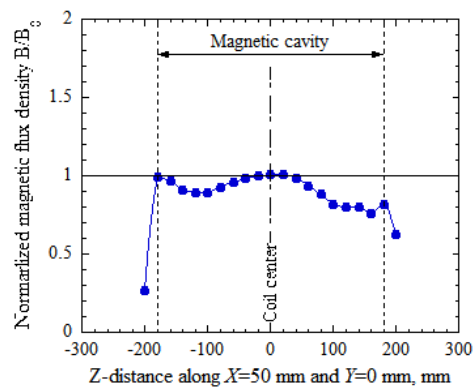
a) (A):  $Y=0$  mm,  $Z=0$  mm



b) (B):  $X=0$  mm,  $Z=0$  mm



c) (C):  $X=50$  mm,  $Z=0$  mm



d) (D):  $X=50$  mm,  $Y=0$  mm

**Figure. 11** Normalized magnetic flux density distributions in the case of 2 kA-coil current.

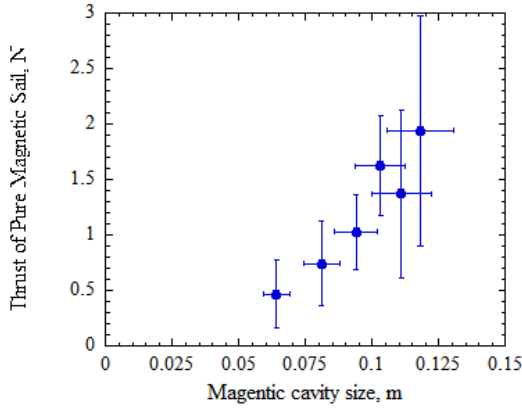


**Figure. 12 Thrust for theoretical cavity sizes achieved from changing of coil current.**

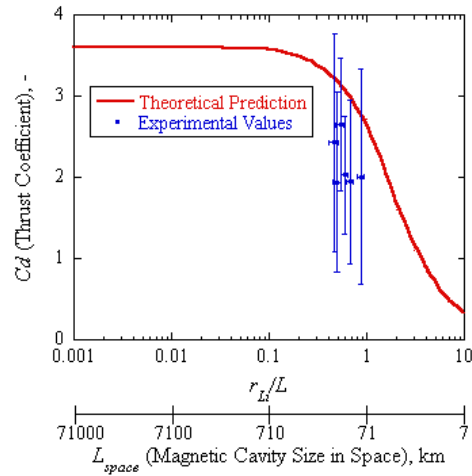


**Figure. 13 Non-dimensional thrust characteristics of Magnetic Sail; theoretical plot is from [v].**

## V. Conclusion

Laboratory experiment of Magnetic Sail was conducted to measure magnetic field around MagSail and thrust of MagSail. The interaction between the simulating solar wind and the coil magnetic field of MagSail was successfully demonstrated in laboratory and it was observed that the size of interaction was changed for the increasing of the coil magnetic field strength, which was controlled by the coil current, in the image of the flow field. The shape of the magnetopause of MagSail was asymmetrical shape. From the result of thrust measurement of MagSail, it is found that thrust was increased for the enlargement of the magnetic cavity size.

## Acknowledgments

We would like to express our acknowledgments to the members of the MPS working group in Japan Aerospace Exploration Agency (JAXA) for their valuable advices. This research is supported by the Grant-in-Aid for Scientific Research (A) 21246126 of the Japan Society for Promotion of Science, and by the space plasma laboratory of ISAS/JAXA.

## References

- <sup>i</sup> I. Funaki. and Y. Nakayama, "Sail Propulsion Using the Solar Wind", The Journal of Space Technology and Science, Vol.20, No.2, 2004, pp.1-16.
- <sup>ii</sup> Willis, D.M., "Structure of the Magnetopause", *Rev. Geophys. Space Phys.*, 9, 953, 1971.
- <sup>iii</sup> Bachynski M. P. and Osborne F. J. F., "Laboratory Geophysics and Astrophysics", in *Advances in Plasma Dynamics* (Anderson, T. P. and Springer R. W. Eds), Northwestern University Press, 1965.

<sup>iv</sup> Yur, G., Rahman, H. U., Birn, J., Wessel, F. J. and Minami, S., “Laboratory Facility for Magnetospheric Simulation”, *Journal of Geophysical Research*, Vol.100, A12, 1995, pp. 23727-23736.

<sup>v</sup> Fujita, K., “Particle Simulation of Moderately-Sized Magnetic Sails,” *The Journal of Space Technology and Science*, Vol. 20, No. 2, 2004, pp. 26–31.